# D8, Bunched efficiency preliminary study - 60 GHz

# Intermediate report on bunched efficiency

Task 9: Beam preparation

Thierry Lamy, Louis Latrasse, and Thomas Thuillier
Laboratoire de Physique Subatomique et de Cosmologie
Université Joseph Fourier Grenoble 1, CNRS/IN2P3, Institut National Polytechnique de Grenoble, 53 Avenue des Martyrs F-38026 Grenoble Cedex, France

# 1 ECR Pulsed ion beam production

## *1.1 PHOENIX 28 for lead Afterglow study*

Electron Cyclotron Resonance Ion Sources are able to produce continuous and pulsed ion beams. The first ECR ion source dedicated to the production of pulsed beams working at 28 GHz has been developed at LPSC: PHOENIX-28 (Figure 1). A plasma is ignited into the plasma chamber by the ECR resonance of the electrons with the RF waves. It is confined by a magnetic structure, the grey iron parts permit to increase the axial magnetic field into the plasma chamber in order to optimize the axial confinement, the hexapole built with permanent magnets insures the radial one (1.2T).The central part of the source (surrounded by the green insulators) is brought to high voltage, a simple grounded electrode (puller of the ion extraction) permits to establish an electric field which accelerate the ions of the plasma and then creates the beam. The classical way and the simplest one to obtain a pulsed beam is to pulse the RF power.

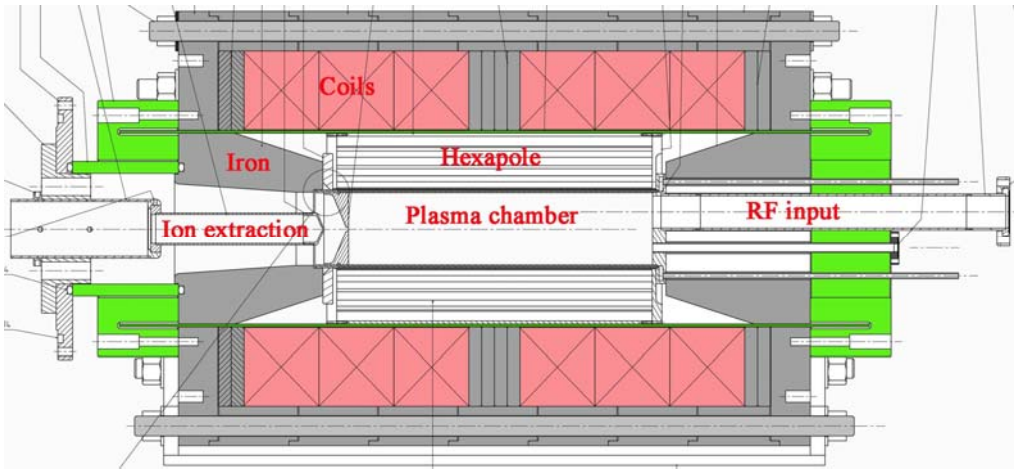


Figure 1: PHOENIX – 28 ECR ion source

This source was developed in order to produce a pulsed lead ion beam suitable for LHC injection, due to the high currents expected (close to 1mA of $Pb^{27+}$), a high current - high transmission beam line has been setup (Figure 2).

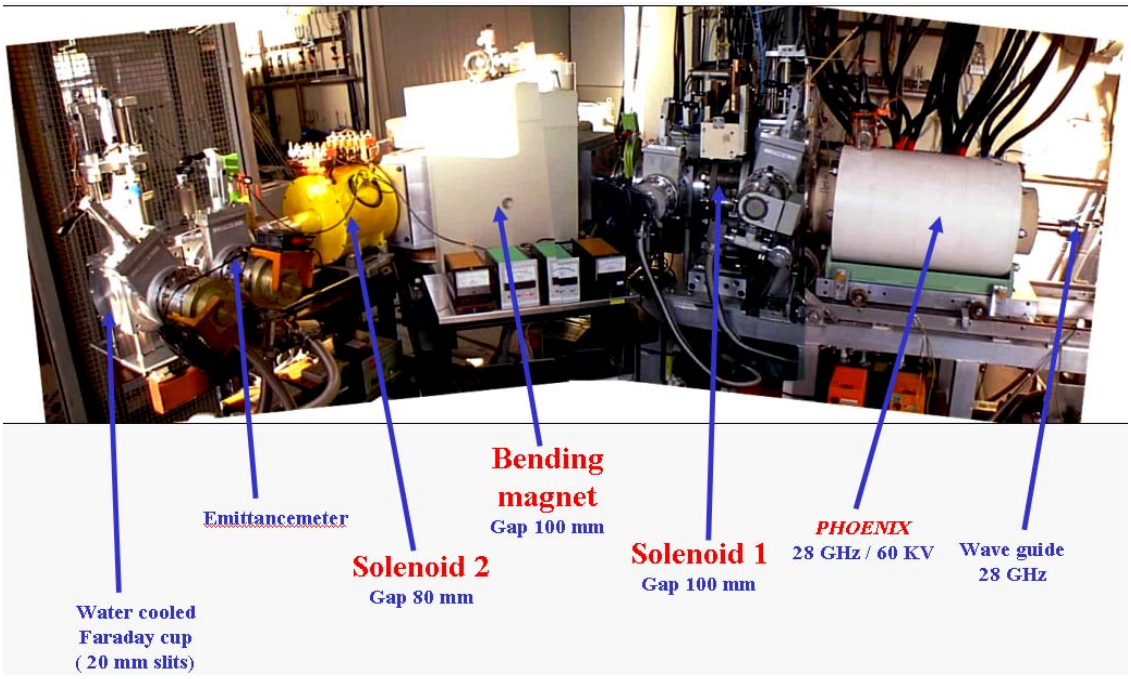


Figure 2: High transmission beam line

## 1.2 Experimental observation of Preglow

In pulsed operation, when the RF pulse stops, we get an afterglow: the plasma is no more sustained, the ions trapped created into the discharge are expulsed due to the destruction of the potential dip. A typical Afterglow signal is shown Figure 3. The yellow and green vertical lines represent the RF pulse beginning and end respectively.

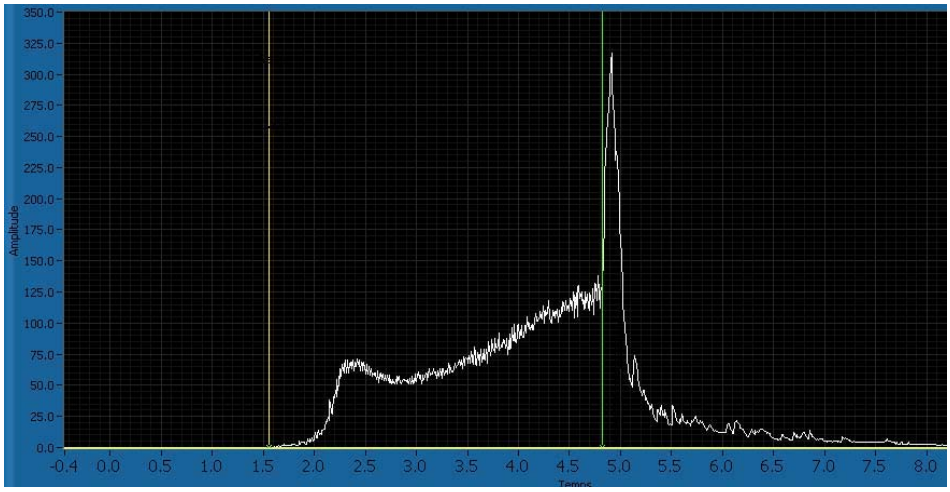


Figure 3: Typical $Xe^{18+}$ Afterglow signal.

The study of such pulsed beam necessitates to perform 3D spectra, a typical lead Afterglow spectrum is shown Figure 4. The X axis is the magnetic field of the bending magnet, the Y axis is the time and the colors represent the intensity of the beam. The increase of the afterglow efficiency for higher lead ion charge states is clearly shown.

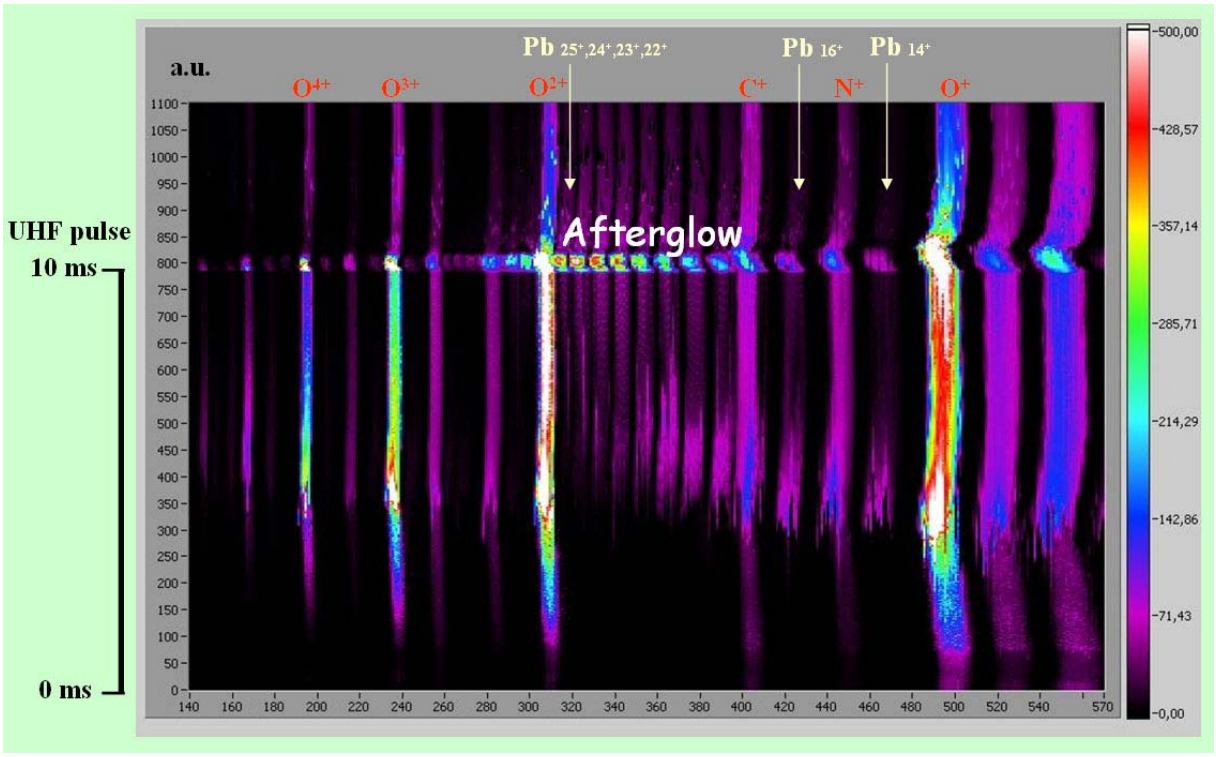


Figure 4: Lead spectrum showing Afterglow at the RF pulse end

During these studies it has been noticed at the beginning of the RF pulse, for some tunings, a fast and intense extracted beam associated to a pressure decrease in the source: this peak has been named the Preglow. In some conditions, the pressure decrease was so important, that after the initial intense ion beam peak extracted, the plasma could not be maintained. Figure 5 schematically shows the experimental observation. In the plasma chamber (~ 2 liters) at $10^{-6}$ mbar, a one decade pressure decrease shows the possibility to extract about $10^{13}$ ions during the pulse.

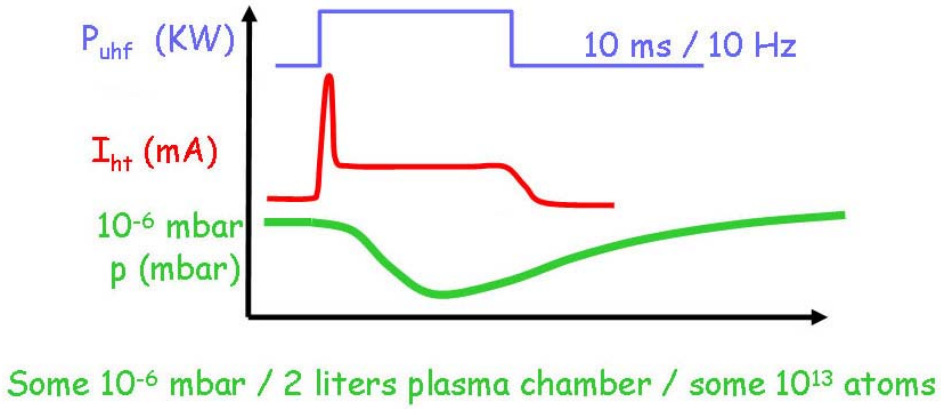


Figure 5: Schematics of the experimental observed Preglow

The first Argon Preglow spectrum obtained with an ECR RF frequency of 28 GHz (1kW) is shown Figure 6. The RF pulse duration is 15 ms with a repetition rate of 4 Hz, the duration of the Preglow signals is roughly 1 ms, the argon charge state distribution is then peaked on the 8+. During the pressure decrease, the discharge is not more able to generate high charge

states, the plasma density is low, the ion intensities extracted as well. This first Preglow obtained, shows that this process allows to produce high intensity fast pulsed beams with average charge states.

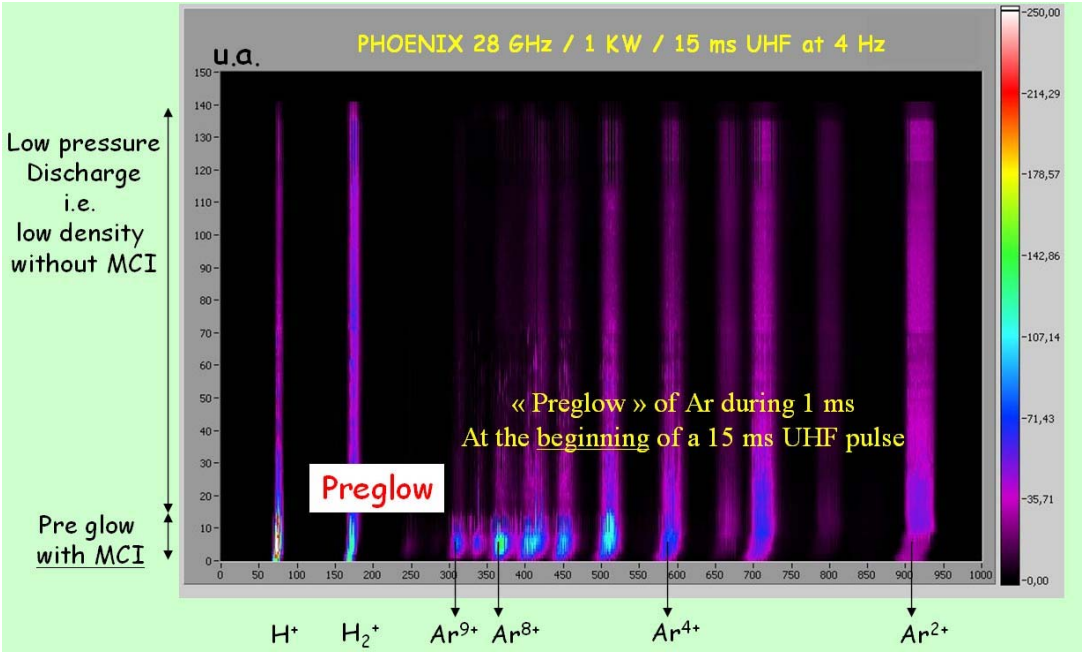


Figure 6: Argon spectrum showing Preglow at the RF pulse start

# 2 Experimental setup

## *2.1 Modified version of PHOENIX 28: PHOENIX V2*

The high efficiency ionisation of a radioactive gas near a radioactive target has consequences on the design of an ECR ion source. The larger the plasma volume, the larger the total current to be extracted and handled at low energy. In case we use a large volume ECRIS, a buffer gas should be injected in the ECRIS to sustain the plasma (even in pulsed mode). So the lower the plasma volume, the higher the ratio of radioactive gas with respect to the buffer gas, and the lower the total current to extract from the source. In order to simulate this situation, a new prototype (PHOENIX V2 – Figure 7) has been designed with a 0.6 liter plasma chamber.

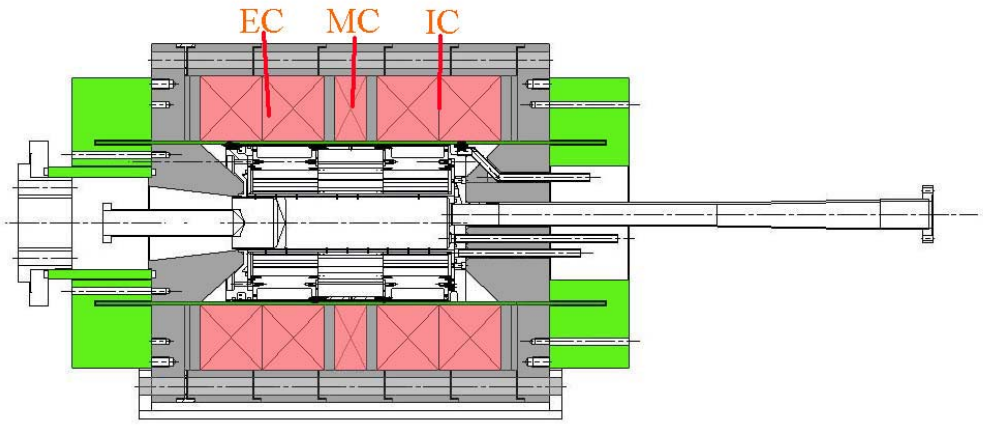


Figure 7: Phoenix V2 ion source

The radial magnetic field increased to 1.35 T, and the axial one is up to 1.6T at the injection side (IC), 1.4T at the extraction (EC) and 0.4T at the middle of the structure (MC). The 18 GHz resonance occurs at a 0.64 T magnetic field, when the 28 GHz one is at 1 T. due to the reduced volume of the source it is difficult to insure the resonance for each frequency maintaining a reasonable mirror ratio.

## 2.2 Preglow experimental methodology

All the systematic Preglow studies have been performed with this PHOENIX V2 source. Specific attention has been paid to the evolution of He and Ne Preglows with respect to different parameters: RF frequency (18 and 28 GHz) and power, support gas nature and pressure, plasma electrode hole diameter. To evaluate efficiencies, a Leybold calibrated leak TL6 ($5\times10^{-6}$ mbar.l.s$^{-1}$) has been used to inject either $_3$He or $_{22}$Ne isotopes. It permits to control the injected neutral flux per second in order to be close to the EURISOL $_6$He and $_{18}$Ne estimated production rates. Figure 8 shows the PHOENIX-V2 test bench with its HV platform and calibrated leak.

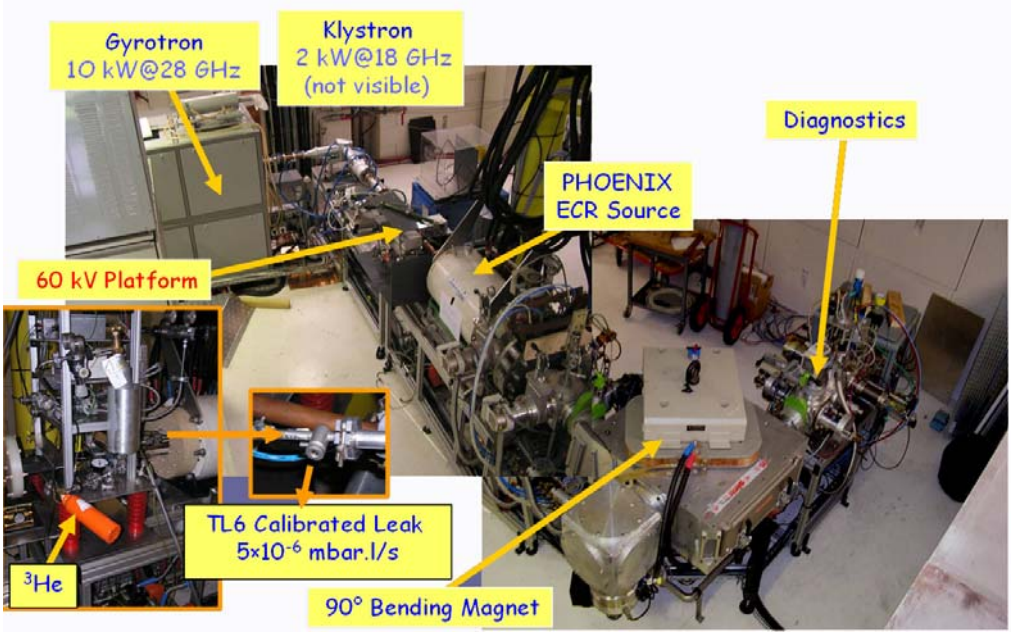


Figure 8: PHOENIX-V2 test stand

# 3 CW ionization efficiency for He and Ne

$_3$He is injected through the TL6 calibrated leak, oxygen is injected as buffer gas (typically $10^{-5}$ mbar), the RF power is 300 W and the extraction voltage 40 kV. The ionization efficiency on a specific charge state is defined as the number of ions per second measured in the faraday cup divided by the number of atoms coming out of the calibrated leak. The ionization efficiency spectrum is shown Figure 9.

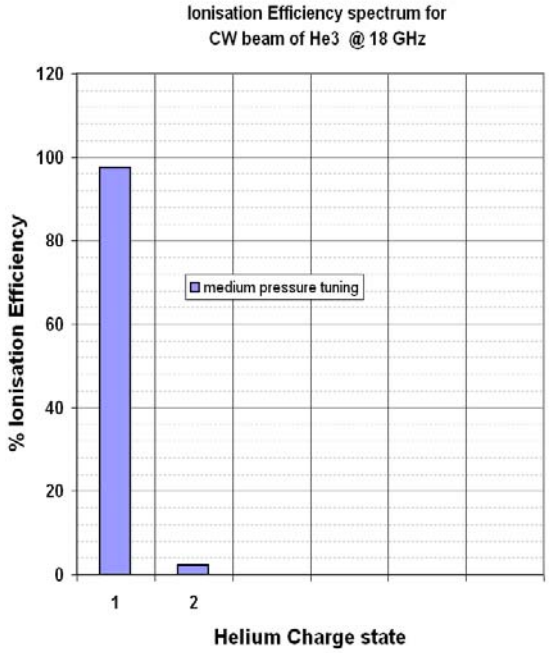


Figure 9: $_{3}$He ionization efficiency spectrum

The global ionization efficiency (sum of the different charge states efficiencies) is 100%, 99% of the ions extracted are in the 1+ charge state, due to the medium pressure and low power tuning.
In case of $_{22}$Ne, $_{4}$He is injected as buffer gas (usual tuning for ECR ion sources), the ionization efficiency spectrum is shown Figure 10 for two buffer gas pressures.

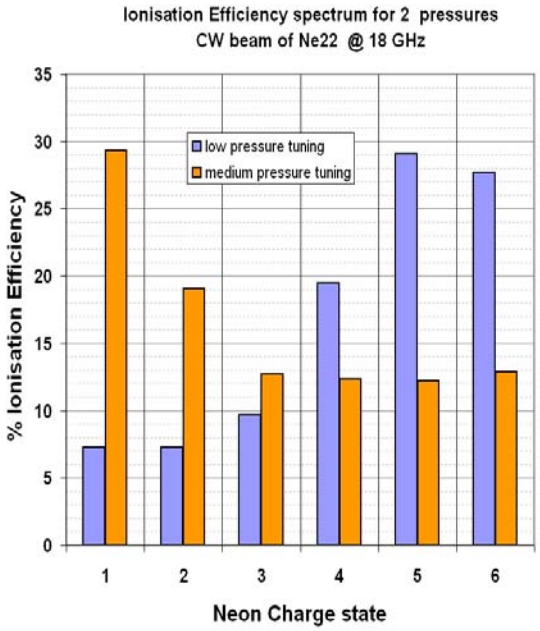


Figure 10: $_{22}$Ne ionization efficiency spectra for two buffer gas pressures

The global ionization efficiency is 100 % as for $_3$He, the pressure of the buffer gas permits to tune the charge state distribution but does not affect the global efficiency. Due to the charge state distribution, the highest efficiency on one charge state is limited to roughly 30 %. The same experiments have shown a much lower global ionization efficiency with the 28 GHz RF frequency (about 25%), in fact, due to the relatively low magnetic confinement of the plasma, the 1 Tesla ECR resonance is very close to the plasma chamber wall and the RF power was limited for safety at 800 W. But in this case the ion extraction time is faster. The optimum axial magnetic field leading to the 100% efficiency was about 1.3 T at 18 GHz, the scaling laws show that the optimum magnetic field at 28 GHz should reach more than 2 T instead of the 1.6 T available.

In the next section, $_{22}$Ne is injected through the calibrated leak, the microwave frequency is 28 GHz, the buffer gas is $_4$He with a typical pressure of $10^{-5}$ mbar, and the extraction voltage is 30 kV. Different charge state distributions for several plasma optimizations are presented on figure 11. As shown on this figure, it was possible to tune each charge state, and this, relatively easily. Indeed, the more influent parameter in the tuning is the microwave power: low microwave power support the production of low charge ions (100 W for $Ne^+$ in this case) and high microwave power support the production of multi-charged ions (600 W for $Ne^{6+}$ in this case).

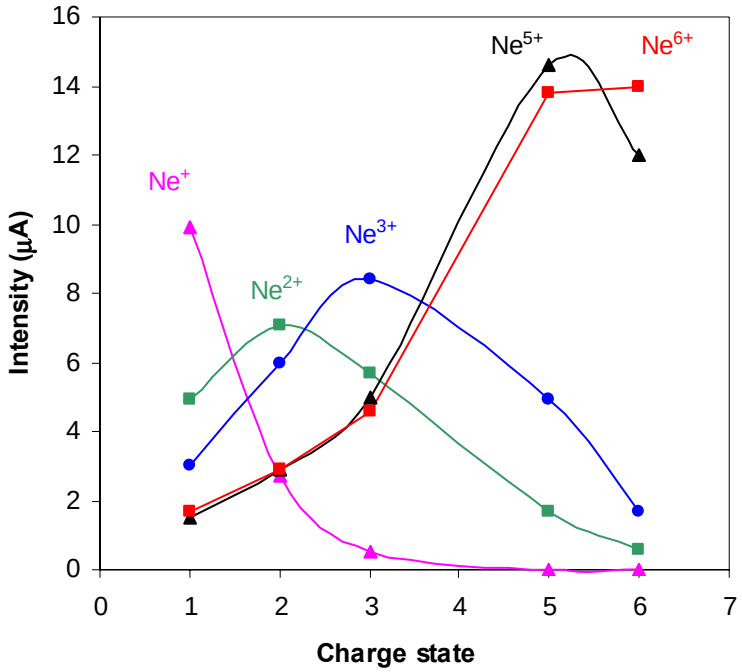


Figure 11: Intensity as a function of the charge state for several charge optimizations

Unfortunately, it was impossible to calculate the ionization efficiency in this case because of a calibration problem of the $_{22}$Ne leak. However, in continuous mode, the variation of the ratio between the intensity and the charge state (I / Q) as a function of the charge state has the same evolution as the ionization efficiency. Thus, figure 12 presents the variations of I / Q as a function of the charge state for the previous tunings. For each tuning, the sum of all the ratios I / Q (considering the 4+ intensity as the average intensity between the 3+ and 5+) is almost constant and ranges between 11.5 and 12 µAp. This result means that the total ionization

efficiency is constant for all tunings. Former experiments, with $O_2$ as buffer gas, have shown a total ionization efficiency of about 75 %. One can notice that for the 1+ charge state tuning, there are only 3 charge states, for other tunings the same number of ions is distributed among 6 charge states, this situation naturally decreases the efficiency on one peak. From these experiments, one can see that the 1+ beam of the $Ne^+$ optimization contains 2 to 3 times more ions than the other charge states beams.

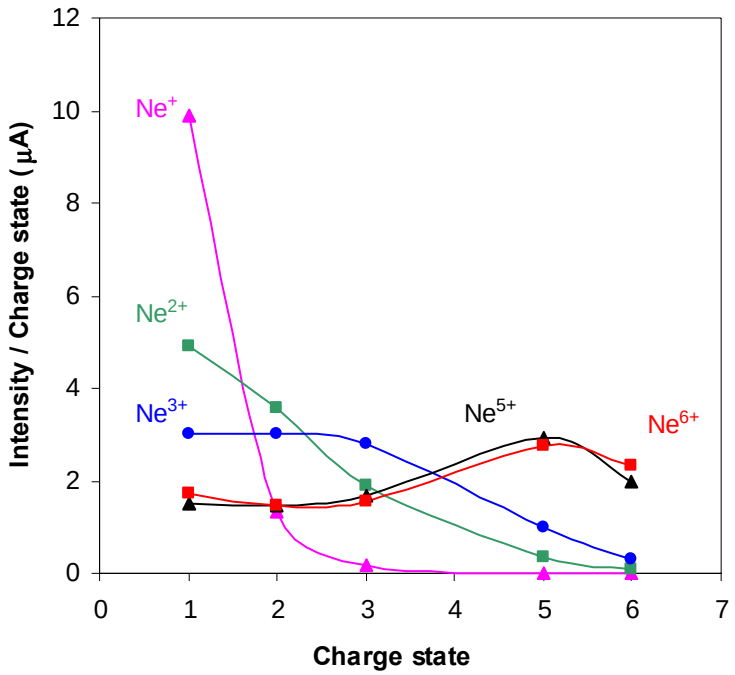


Figure 12: Variations of I / Q as a function of the charge state for several tuning

# 4 Preglow Analysis for Helium

## *4.1 Magnetic confinement and heating frequency influence*

Two different pulsed RF waves have been successively axially injected in the PHOENIX V2 ECR source. The first one is generated by a 2 kW 18 GHz klystron, while the second comes from a 10 kW 28 GHz gyrotron. Between the two experiments one can consider, due to the ECR scaling laws, that the critical plasma density is increased by a factor of $(28/18)^2 \approx 2.4$, however due to the limited magnetic structure characteristics, one may consider too, that the confinement time is not the same for these two plasma heating frequencies. Figure 13 reports the difference observed between the pulse shapes at 18 and 28 GHz for $_3$He beams. The high magnetic confinement at 18 GHz gives a large preglow Full width at half maximum (FWHM) and a very long afterglow tail that continues up to the next pulse (10 ms, 10 Hz in this experiment). It means that a lot of ions are lost between two RF pulses. The low magnetic confinement studied with 28 GHz RF heating changes the pulse shape : the preglow is more narrow, the peak intensity is maintained to the level of the 18 GHz thanks to higher microwave power, and the afterglow tail is much less important than at 18 GHz. The width of the preglow signal is much shorter when injecting 28 GHz (typically 200 µs), that means

about 4 times shorter than the average pulse length at 18 GHz. When increasing the frequency to 60 GHz, the additional density increase should shorten more the process evolution.

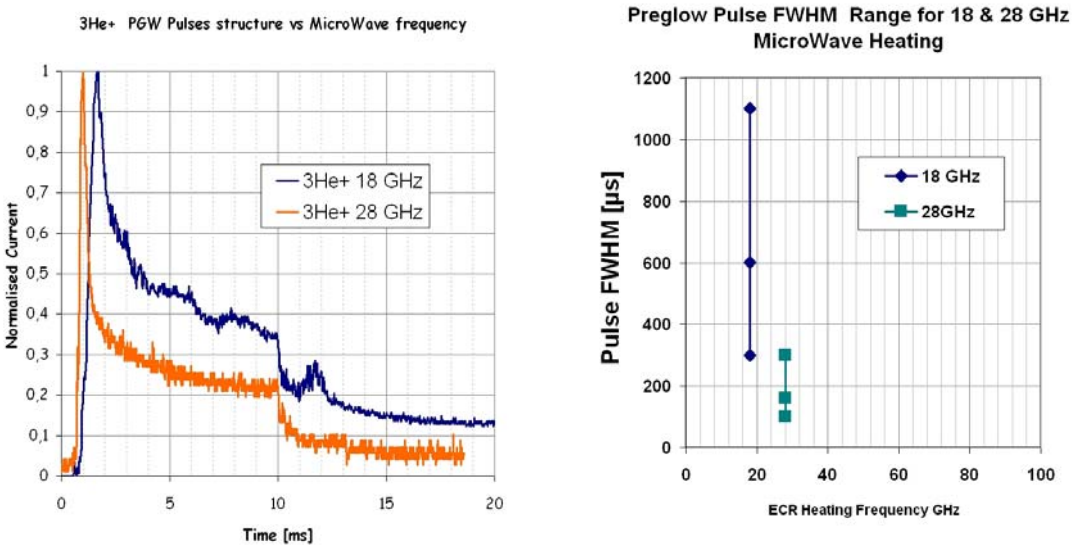


Figure 13: Influence of the RF heating frequency on the Preglow time structure

## 4.2 Buffer gas flux influence

These experiments have been first done with the 18 GHz Klystron. Considering like said in 2.2, the helium flux being constant, the $_3He^+$ and $_3He^{2+}$ intensities are a direct and relative image of the ionization efficiency in the preglow. When increasing the $_4He$ buffer gas flow we observe a decrease of the preglow intensity, like seen in Figure 14. The decrease is linear on a significative range and the loss rate is the same for the 1+ and 2+ charges. The lower buffer gas flux experiment was reached when the $_4He$ valve was closed. It means that the remaining $_4He$ peak intensity was due to the residual pressure in the source and was mainly $O^{4+}$ and $C^{3+}$. It is clear that a higher preglow intensity could be obtained with a better vacuum in the source. The vacuum in PHOENIX V2 is limited by the use of Perbunan O-rings and a Fortal plasma chamber that produces non negligible outgasing. For future experiments, one should consider to use a stainless steel plasma chamber and Conflat flanges for the source and the beam line to minimize impurity partial pressures.

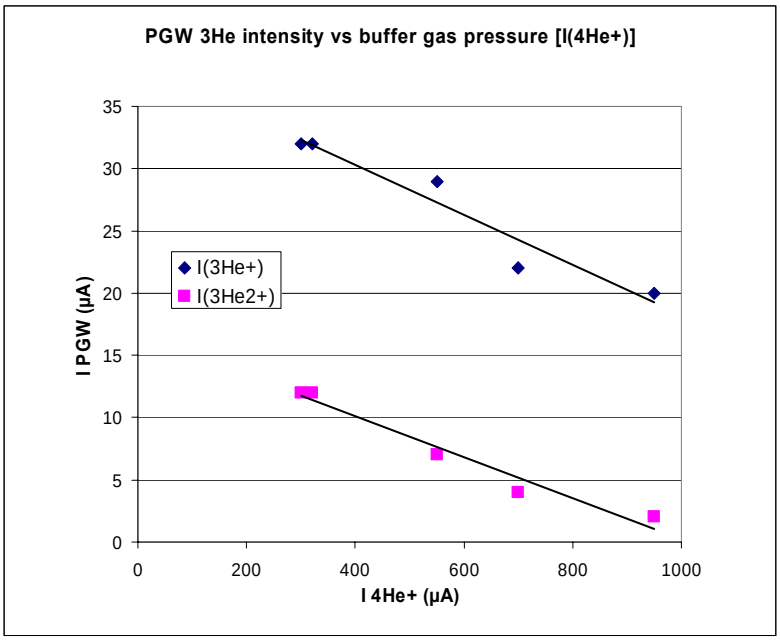


Figure 14: efficiency variation with the buffer gas pressure

Figure 15 reports the evolution of the Preglow FWHM with the buffer gas pressure. Once again, the pressure has an important effect: One can see that the FWHM is increasing with the pressure, especially for the 1+ charge state. For high pressures on can see saturation for the FWHM and the Preglow intensity above 800 µA of 4He current, in fact the preglow peak vanishes and a classical ECR rising pulse takes place.

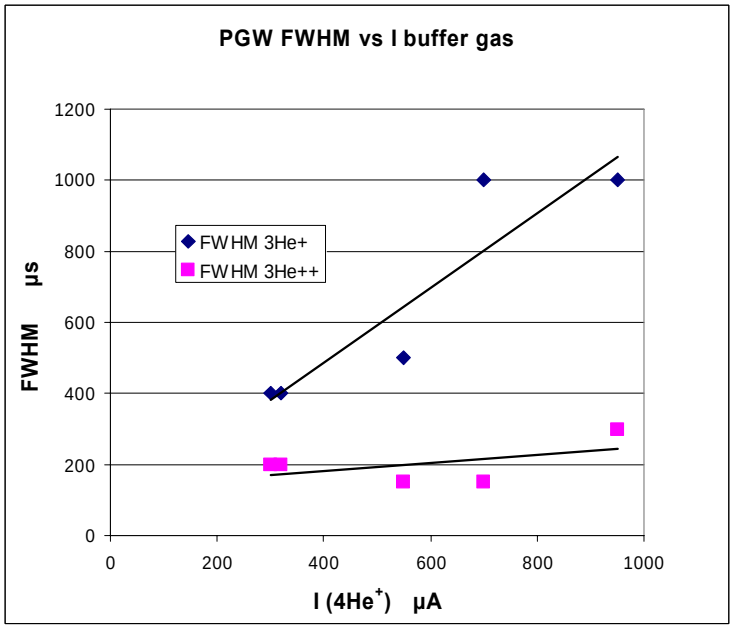


Figure 15: Preglow FWHM versus buffer gas pressure

## 4.3 Microwave parameters influence

The microwave parameters are the power level, the pulse frequency and the pulse length. Their tuning are very sensitive in pulsed mode since they enable to modify accurately the equilibrium pressure in the plasma chamber. They have an effect on the pulse shape and the ion charge state distribution.

***Duty Cycle variation***

Given the pulse frequency and pulse power level, the change of the pulse duration often enables to find an intensity optimum. As an illustration, a duty cycle study has been performed for $_3He^+$ production at 18 GHz with 10 Hz pulse frequency and a fixed power intensity of 500 W. The variation of the preglow intensity (orange curve) and FWHM (blue squares) with the pulse length is plotted on figure 16. One can see, for this study, that the preglow FWHM increases from 800 µs to 3 ms when the duty cycle increases from 0.1 to 0.5 and an optimum preglow intensity is reached for 25 ms pulses.

An Argon study has been performed too at 18 GHz, a Preglow was obtained for charges from 2+ to 4+ and the FWHM was in the range 0.3 to 0.8 ms when increasing the RF power.

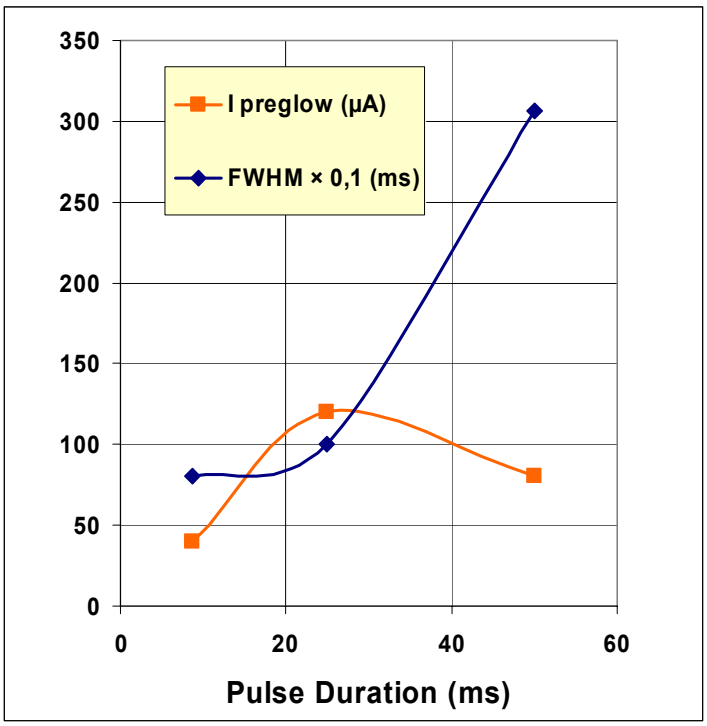


Figure 16: $_3He+$ preglow intensity and FWHM evolution at 18 GHz, 10 Hz, for several pulse durations (note that FWHM has been divided by ten for convenience)

***Pulse repetition rate variation***

Another investigation was done with the 28 GHz gyrotron. In this experiment, the RF power was fixed to 4kW and the pulse length to 10 ms. The plasma electrode hole diameter was set to 2 mm in order to minimize the $_3He$ gas loss pumped through the plasma electrode to the turbomolecular pumps. The pulse repetition rate was varied from 5 to 30 Hz, this last value being the upper limit of the main high voltage power supply of the gyrotron. The resulting evolution of the preglow intensity for 1+ and 2+ charge states is plotted on figure 17.

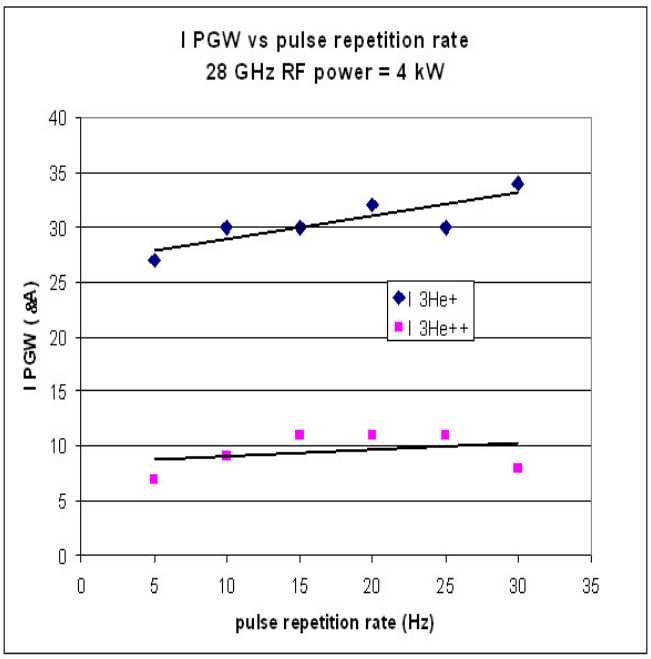


Figure 17: $_3He^+$ and $_3He^{2+}$ Preglow intensity as a function of the RF repetition rate

It is very interesting to note that the preglow intensity remains constant and even increases for 3He1+ with increasing pulse rate. One can notice a slight decrease of 3He2+ preglow intensity for high repetition rate. This is the consequence of the mean power increase deposited in the plasma chamber generating new transitory outgasing flux from the plasma chamber wall. This outgasing is expected to decrease with time. Finally, in a longer experiment one should expect to see both He1+ and He2+ increase with pulse repetition rate. The low magnetic confinement of PHOENIX V2 28 GHz has for consequence that the plasma vanishes rapidly after the microwave pulse ends and there is no plasma memory from pulse to pulse.

On the range studied, the repetition rate is increased by 6, so per time unit, we extract 6 times more peaks, due to the constant flux given by the calibrated leak, we have naturally increased the global ionization efficiency by a factor 6 at least. This is a very important point for EURISOL, if the repetition rate of the accelerators can be increased, the efficiency of the neutrino production will be proportionally increased.

***Microwave power variation***

The microwave power study has been carried out at 18 and 28 GHz. The analysis of the results has to be carefully performed, since the power increase may generate some impurity superposition, for example $_{12}C^{4+}$ which has the same Q/A than $_3He^{1+}$. The method to evaluate the carbon ions level during the $_3$He preglow is to first check the intensity of the carbon lower charge states, and second, to check the level of the afterglow which is much efficient for multicharged ions than for singly charged ones. Figure 18 shows a quasi linear increase of the Preglow levels from 500 to 2000 W for the 18 GHz RF frequency input. No current saturation is reached and a higher microwave power may result in higher peak current performances. This curve was achieved with a 8 mm plasma electrode hole diameter.

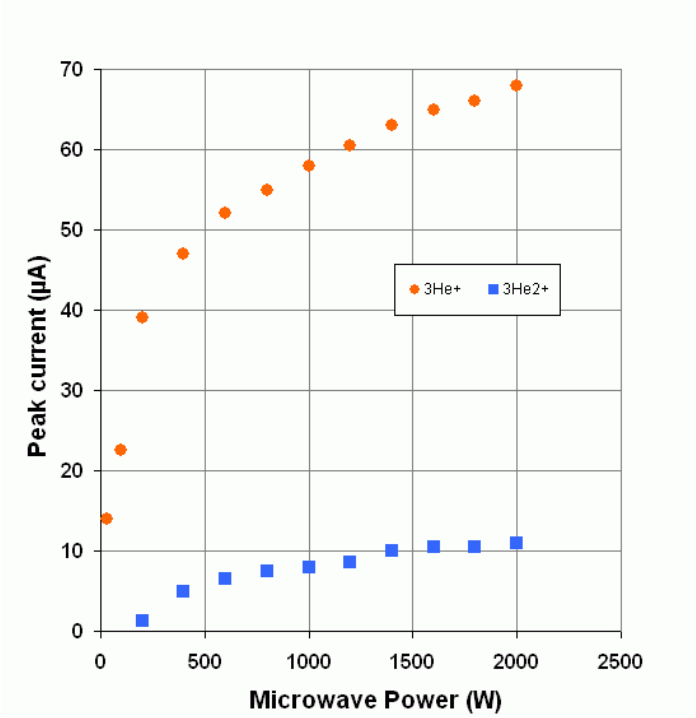


Figure 18: Preglow intensities for He+ and He2+ versus 18 GHz RF power

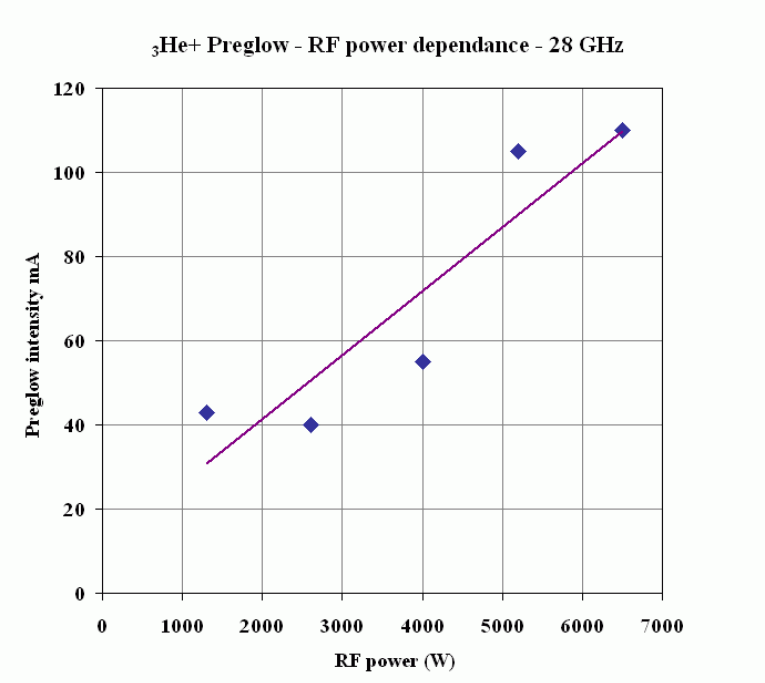


Figure 19: He+ Preglow intensity versus 28 GHz RF power

Figure 19 shows the same evolution for a 28 GHz RF frequency input from 1 to 7 kW.
To limit pumping through the extraction electrodes holes between each RF pulse, the plasma electrode diameter was set to 4 mm. One can see a quasi linear increase of the preglow intensity with the microwave power increase like in the 18 GHz experiment. For power above 5 kW, where best performances are reached, a very high total current, around 10 mA, was

extracted from the source. The advantage of a small diameter hole is to keep the useful He gas in the source in order to bunch it during the RF power pulse, but the consequence is a pressure increase in the source. Also one should not forget that at high power there is an additional outgasing contribution from the plasma chamber walls (in the case of the Fortal plasma chamber of PHOENIX-V2). Hence, an extraction limitation was observed for the high power tuning since the total extracted current was above the Child-Langmuir limit of our simple diode extraction system (40 kV).

## *4.4 Summary and Insight of Bunching Ionisation efficiency studies*

Experimental investigations performed at 18 and 28 GHz enabled to better understand the way to produce high efficiency pulsed beam.

First, the plasma contamination with C, N, O coming either from Perbunan O-rings, or outgasing from the Fortal plasma chamber wall has considerably complicated the analysis of the ions spectra. In real operation condition near a radioactive target, C,N,O will anyway come from the target with Ne or He, so these difficulties will remain, but it appears to be mandatory to design a UHV beam line and UHV ion source using copper gaskets and material having low outgasing properties (like stainless steel) in order to minimize this contamination.

Second, the CW and pulsed tests performed for Neon and Helium clearly show that the highest ionisation efficiencies are reached for low ion charge states. Say differently there are more ions per charge state peak when the same number of ions is shared among a few peaks than among a full multicharged ion spectrum. The production of low charge state plasma offers the advantage to limitate risks of ion beam contaminations since the beams are more separated through a magnetic analysing bending magnet. A special care should be taken to keep a high plasma density at the same time as a low charge state distribution plasma. This kind of compromise can be obtained with a not too high magnetic confinement and a high power, high frequency microwave generator, like a 60 GHz/100 kW one.

Third, the best results were obtained for high total current extracted from the source, so a particular care should be taken to the ion extraction system. In real production conditions, the total current extracted from the source will even be higher, assuming a 60 GHz microwave heating and non negligible C,N,O contamination from the target. A 100 kV platform should be considered as a minimum for high voltage extraction. In order to minimize total current to be extracted, the buffer gas flow should be minimized with respect to the rare gas flow of interest. The solution is to build a plasma chamber with a volume as small as possible in order to make the usefull Ne or He atoms proportion as high as possible with respect to other atomic species.

The experimental ionisation efficiency was measured as the number of ions included in the preglow peak, taking into account the available experimental FWHM. At best, the 18 GHz experiments enable to reach a 10 % ionisation efficiency for He+ at 10 Hz, but with a FWHM around the millisecond. So the real useful efficiency for beta beam during 100 µs is reduced by a factor ten down to 1-2 %. The best result achieved with 28 GHz was 1% per 10 Hz repetition rate, with a FWHM equal to 300 µs. So the ionisation efficiency at 30 Hz is 3%, and the useful efficiency contained in the 100 µs time structure is also 1-2 % in this case.

# 5 Preglow study for Neon

The Neon experiments have been done with $_{22}Ne$ isotope. The presence of the C, N, O ions in the ECRIS renders impossible a confident analysis of charge states 4,7,8,9 due to superposition of the A/Q issued from the magnetic spectrometer. For this study, the microwave frequency is 28 GHz and the buffer gas is $_4He$ (typically $10^{-5}$ mbar) and the extraction voltage is 30 kV. Ne ion pulses are presented on figure 20. In this case, the microwave power is 1500 W, the pulse duration is 6.5 ms and the pulse frequency is 10 Hz.

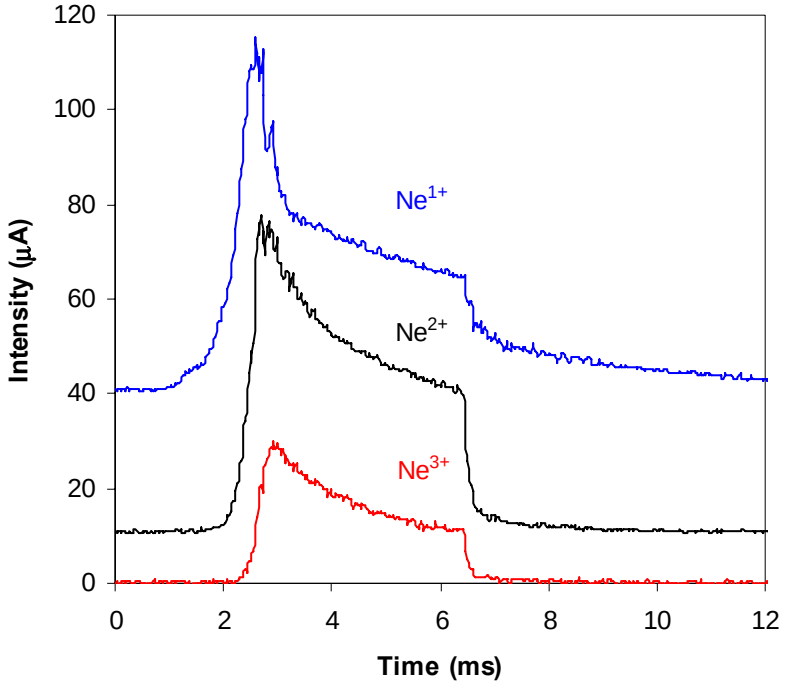


Figure 20: Ne intensity pulses, the pulse duration is 6.5 ms and the pulse frequency is 10 Hz

For different charge states we measured the FWHM, the time to reach the intensity maximum, the increase time which is defined as the time it takes to increase the intensity from 10 % up to 90 % of the intensity maximum of the Preglow peak and the time to reach 10 % of the intensity maximum of the preglow peak. The results are presented on figure 21.

One can notice that the time of the intensity maximum and the time to reach 10 % of the intensity maximum, which represents the creation time of the concerned species, increase with the charge state. Indeed, the more the charge increases, the more time is needed to create this species. Moreover, there is a slight decrease of the FWHM and of the increase time, which are lower than 1 ms, for increasing charge states. However, experiments with argon have shown that the FWHM and the increase time are almost constant for a charge state range between 2 and 9. More systematic measurements should be performed.
Former experiments, with $O_2$ as buffer gas and at a fixed charge state, have shown that all these preglow parameters decrease when increasing the microwave frequency.

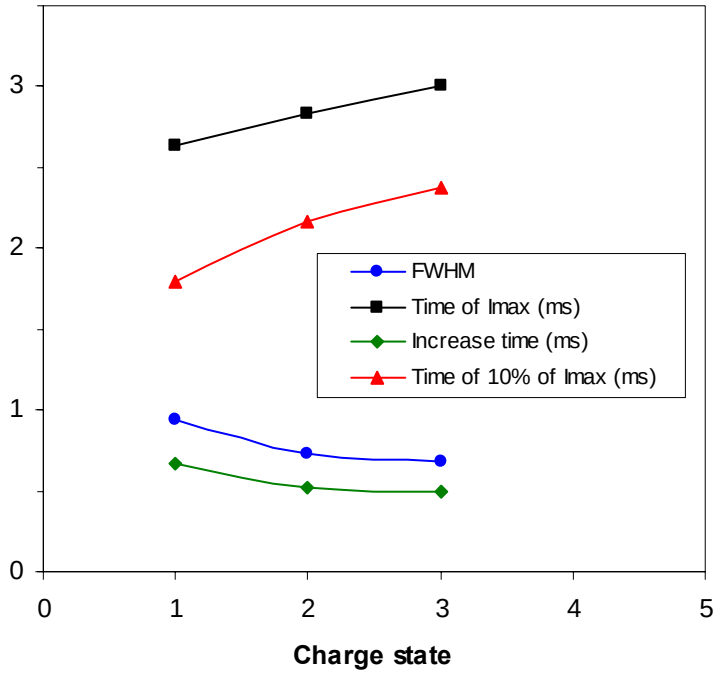


Figure 21: Variations of the FWHM, the time of the intensity maximum, the increase time and the time to reach 10 % of the intensity maximum of the preglow peak as a function of the charge state.

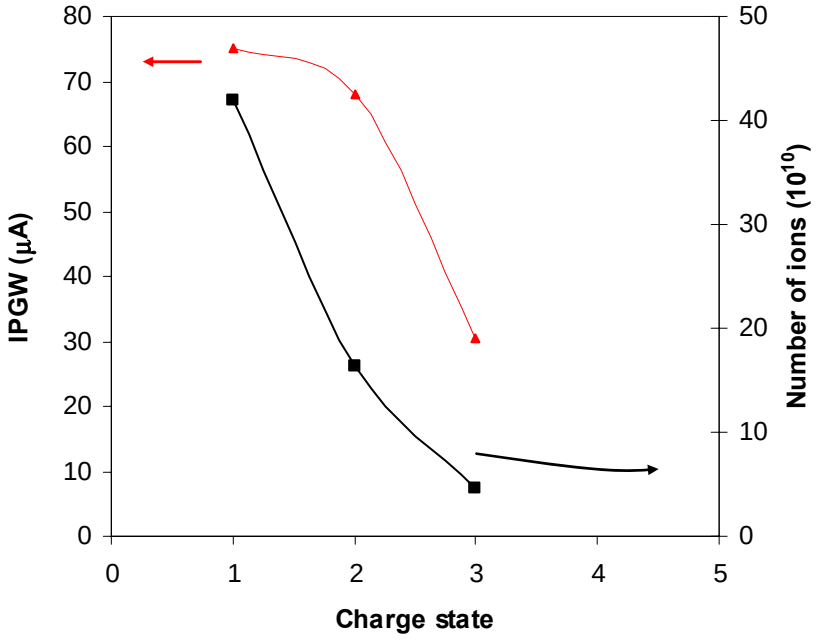


Figure 22: Preglow intensity peak and number of ions in the preglow peak as a function of the charge state

The Figure 22 presents the preglow intensity peak IPGW and the number of ions in the preglow peak as a function of the charge state. The variation of the number of ions in the preglow peak as a function of the charge state has the same evolution as the ionization

efficiency. If we neglect charge states higher than 3, we can give an estimation of the percentage of ions. Thus, the values of the figure 22 give about 67 % of $Ne^{+}$ and 26 % of $Ne^{2+}$. With a different tuning, particularly when decreasing the microwave power from 1500 to 600 W, it is possible to obtain 88 % of $Ne^{+}$.
Experiments, with $O_2$ as buffer gas and with a $Ne^{2+}$ tuning, have shown a total preglow ionization efficiency higher than 5 %. At 18 GHz, the efficiency was about 3%.

# 6 Discussion and prospects

## *6.1 Discussion*

Experimental evidence for Preglow phenomenon has been established. It is interesting to notice that simulation has been performed by physicists from the Institute of Applied Physics in Nizhniy Novgorod (Russia) within the frame of an International Scientific Collaboration Programme between IAP and LPSC. The simulation supposes a classical confinement (Pastukhov), the free adjustable parameters are the initial gas density, the initial electron density, the microwave absorbed power and the transversal confinement time. The best coincidence between experimental results and the simulation, suppose a transversal confinement time of the same order than the longitudinal one, the steady state electron energy is about 10 keV, and the steady state electron density is about 1,2 $10^{10}$ $cm^{-3}$. These parameters are not so far away from the supposed characteristics of classical ECR plasmas, a more detailed study with Argon will be published at the next ICIS conference in Korea (ICIS'07).

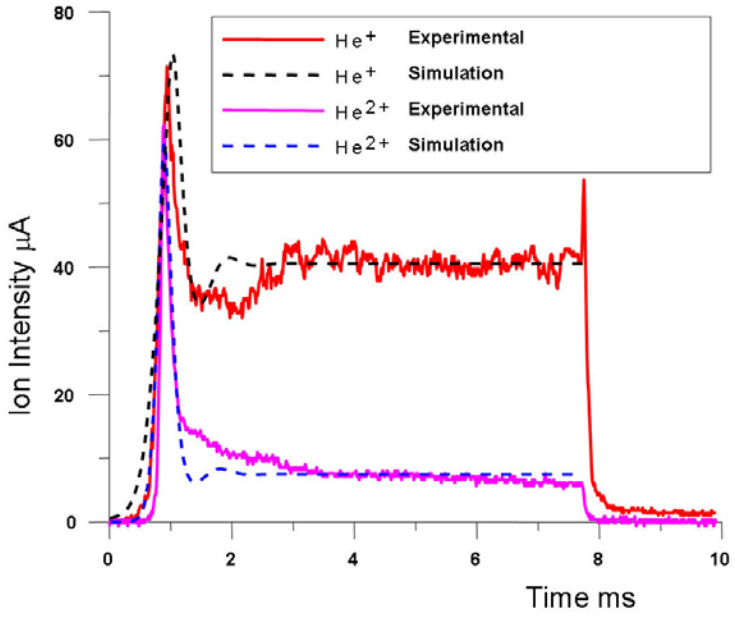


Figure 23: simulation of experimental Preglow

The frequency increase from 18 to 28 GHz has shown better Preglow characteristics especially with respect to time, the Preglow intensity for the 18 GHz or 28 GHz RF input increases with respect to the microwave power without a limitation so far. A better confinement with an improved magnetic field for the 28 GHz experiments should permit to obtain more reproducible results.

## *6.2 Prospects*

### 6.2.1 A-PHOENIX construction

In the Preglow study, it has been emphasised that it was difficult to have a confident study of the pure preglow phenomenon, the experimental limitation being the poor magnetic confinement of the PHOENIX-V2 source for a 28 GHz microwave heating frequency. A new prototype dedicated to a high ion current production (1mA $Ar^{12+}$) has been designed (A-PHOENIX, Figure 24) and built (Figure 25).
The characteristics of A-PHOENIX are the following:
The axial magnetic field is generated by two High Temperature Superconducting coils and a classical one permitting to generate 3T at the injection, 0.6T in the middle and up to 3T at the extraction, the radial field accessible is in the range from 1.6 to 2.1 T and is insured by 3 permanent magnet hexapoles whose magnetic induction is reinforced by soft iron liners welded on the plasma chamber. The plasma volume will be about 1.5 liter.

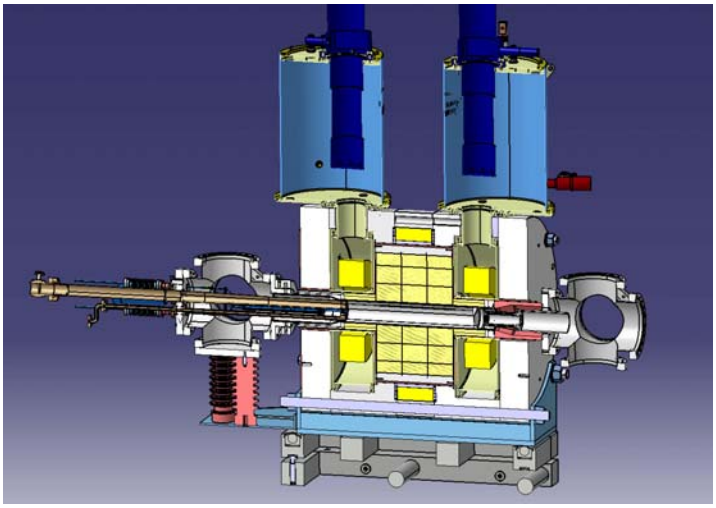

Figure 24: A-PHOENIX design

Figure 25 : A-PHOENIX on the test stand

This new prototype will permit us to overcome the low magnetic field confinement problem of PHOENIX-V2, the previous results given in cw and Preglow mode will be investigated at the 18 and 28 GHz frequencies.

### 6.2.2 60 GHz ECRIS prototype 1 design

We will go through two steps to build the 60 GHz prototype, a first prototype will consist in a simple axial mirror trap when the second one will have a radial confinement. It has been shown before, that to reach high efficiencies, a small volume ion source with an efficient magnetic confinement was desirable. Due to the high extracted currents expected, a specific effort should be performed on the extraction system, a 100 kV insulation will be necessary.

For the construction of the high magnetic field, we collaborate with a HMFL group in Grenoble who uses two main technologies, the Bitter and the polyhelix technique. The elementary part of a Bitter magnet shown in Fig. 26 is a plate of highly pure copper in which the electrical current flows. The plates are stacked and pressed together with intermediate thin insulating layers of polyimide (eg. Kapton). In this manner each plate (or plates in parallel) forms a turn of the winding.

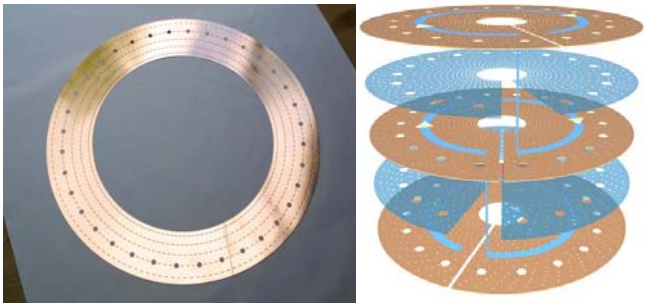

Figure 26: Bitter disk and Bitter assembly. The inner diameter is 400 mm. The cooling slits are 800 µm large. Disks are made of oxygen free copper with 400 MPa yield strength with a minimum conductivity of 100 % IACS.

Preliminary calculations have shown that it was possible to produce a mirror field with two maxima of 4 and 7 Teslas distant of 200 mm with 3 coils like shown on Figure 27.

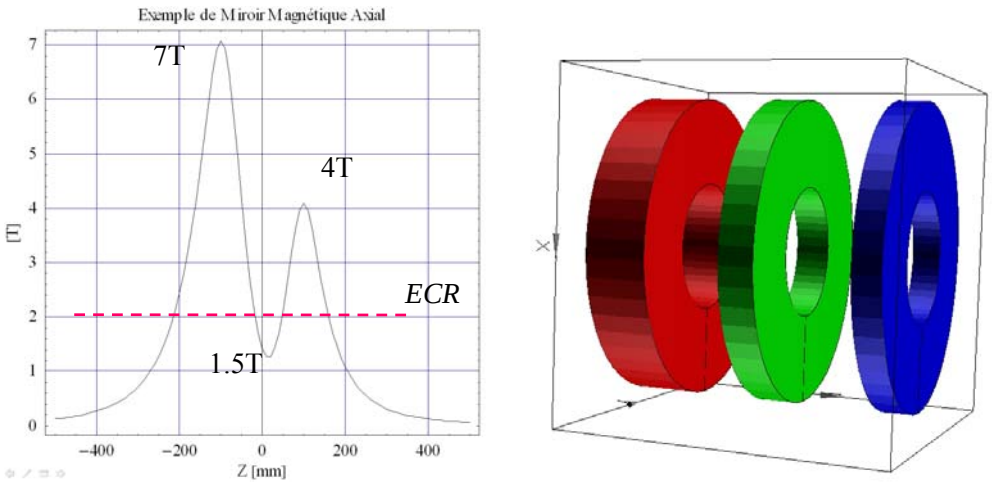


Figure 27 : Preliminary calculation for a 3 coil geometry

A different approach shows the possibility to get two maxima at 4 and 6 Teslas distant of 150 mm with a unique Bitter stacks with variable current density. The detailed study of the axial configuration will be performed during autumn 2007.
The 60 GHz. prototype will take benefits of the advantages of these high field winding techniques in term of:

- **Compacity** : thanks to the high heat transfer coefficient obtained in the thin slit of cooling it is possible to enhance the current density up to 30 000 A/cm$^2$. In addition the thickness of the insulation can be restricted to only 50 µm when using Kapton or even thinner using ceramic coating.

- **Reliability**: to produce high field, it is necessary to optimize the Bitter disks so that the Lorentz forces applied are about 90 % of the yield strength. In the framework of this project we will be able to lower this value down to around 50 %. This is a classical value for the use of copper in mechanical construction, it will then allow making reliable prediction concerning the life duration of the final stack. As compared to classical winding technique the high cooling rate authorized by the Bitter techniques helps to minimize the thermal longitudinal gradient generating additional stress to the magnet.

- **Versatility**: at the contrary of classical impregnated coils, the Bitter techniques allows a step by step development as it is possible to restack easily and then to adjust the current density by playing with different parameters such as plate thickness, number of plates in parallel, addition of blank discs with zero current density, easy change of the overlapped contact surfaces between two consecutive discs.

### 6.2.3 60 GHz ECRIS prototype 2 design

Different technical approaches are under consideration for the radial magnetic field, either bitter coils of a classical shape as shown Figure 28, a more sophisticated structure (Figure 29) permits to generate within the same time axial and radial field.

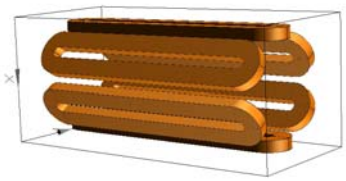

Figure 28: Bitter coil Hexapole structure 1

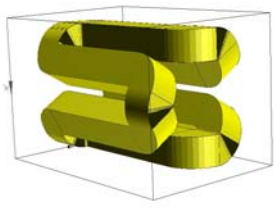

Figure 29: Hexapole structure generating axial field